The EMBO Journal (2008) 27, 2293–2304 | © 2008 European Molecular Biology Organization | All Rights Reserved 0261-4189/08
www.embojournal.org

THE EMBO JOURNAL

Dopamine D2 receptors form higher order oligomers at physiological expression levels

Wen Guo[1,2,6], Eneko Urizar[1,2,6], Michaela Kralikova[1,2], Juan Carlos Mobarec[4], Lei Shi[5], Marta Filizola[4] and Jonathan A Javitch[1,2,3,*]

[1]Center for Molecular Recognition, College of Physicians and Surgeons, Columbia University, New York, NY, USA, [2]Department of Psychiatry, College of Physicians and Surgeons, Columbia University, New York, NY, USA, [3]Department of Pharmacology, College of Physicians and Surgeons, Columbia University, New York, NY, USA, [4]Department of Structural and Chemical Biology, Mount Sinai School of Medicine, New York, NY, USA and [5]Department of Physiology and Biophysics and the Institute for Computational Biomedicine, Weill Medical College of Cornell University, New York, NY, USA

G-protein-coupled receptors are generally thought to be organized as dimers; whether they form higher order oligomers is a topic of much controversy. We combined bioluminescence/fluorescence complementation and energy transfer to demonstrate that at least four dopamine D2 receptors are located in close molecular proximity in living mammalian cells, consistent with their organization as higher order oligomers at the plasma membrane. This implies the existence of multiple receptor interfaces. In addition to the symmetrical interface in the fourth transmembrane segment (TM4) we identified previously by cysteine (Cys) crosslinking, we now show that a patch of residues at the extracellular end of TM1 forms a second symmetrical interface. Crosslinking of D2 receptor with Cys substituted simultaneously into both TM1 and TM4 led to higher order species, consistent with our novel biophysical results. Remarkably, the rate and extent of crosslinking at both interfaces were unaltered over a 100-fold range of receptor expression. Thus, at physiological levels of expression, the receptor is organized in the plasma membrane into a higher order oligomeric structure.

The EMBO Journal (2008) **27,** 2293–2304. doi:10.1038/emboj.2008.153; Published online 31 July 2008
Subject Categories: signal transduction
Keywords: BRET; crosslinking; dopamine; GPCR; higher order

Introduction

G-protein-coupled receptors (GPCRs) comprise a diverse, well-studied system for transducing signals from the extracellular milieu to a variety of intracellular signalling molecules (Bartfai *et al*, 2004). GPCRs have been inferred to be dimers in the plasma membrane (Pin *et al*, 2007; but see Chabre *et al*, 2003; Chabre and le Maire, 2005; James *et al*, 2006; Meyer *et al*, 2006). Class C receptors form homo- and heterodimers but have been inferred not to be organized as higher order oligomers (Brock *et al*, 2007). In contrast, several lines of evidence have suggested that class A receptors might exist as higher order oligomers, although this remains controversial (Chabre *et al*, 2003).

Despite an explosion of recent interest, our understanding of the structural details and functional role of GPCR oligomerization is still limited. Most importantly, it has not been established whether activation of class A rhodopsin-like GPCRs is affected by their organization in a particular quaternary structure. Recently, both rhodopsin (Bayburt *et al*, 2007) and β_2-adrenergic receptor (B2AR) (Whorton *et al*, 2007) have been shown to signal efficiently to G proteins when reconstituted into lipid nanodiscs containing only a single receptor. Thus, after solubilization and reconstitution, these GPCRs *can* function alone. However, whether in fact they do function alone *in vivo* cannot be addressed by such studies and requires an exploration of their native organization.

Much evidence indicates that class C receptors exist and function as homo- or heterodimers (reviewed in Pin *et al*, 2003). Findings in class A glycoprotein hormone receptors support the existence of trans- as well as cis-activation (Ji *et al*, 2002), which requires them to be organized at least as dimers. In addition, ligand binding to one protomer in a GPCR dimer appears to be sufficient to cause an activation-like conformational change in the unoccupied protomer (Damian *et al*, 2006; Brock *et al*, 2007), consistent with transfer of information between the protomers and thus with a functional role of dimerization.

An understanding of the structural basis of crosstalk between receptors must include their interfaces, but information about these interactions is still limited. In various class A receptors, cysteine (Cys) crosslinking studies have supported a contribution of transmembrane 4 (TM4) (Guo *et al*, 2003, 2005; Klco *et al*, 2003; Kota *et al*, 2006) or TM1 and TM2 (Klco *et al*, 2003) to a symmetrical interface. FRET studies performed in the alpha-factor yeast GPCR supported a contribution of TM1 to the dimer interface (Overton and Blumer, 2002). Work with peptides and receptor fragments has supported a contribution of TM1, TM4 and/or TM6 to interaction surfaces (Hebert *et al*, 1996; Ng *et al*, 1996; Baneres and Parello, 2003; Carrillo *et al*, 2004). Recently, a role for TM4 as part of a dimerization interface has been extended to the class B secretin-like class of GPCRs (Harikumar *et al*, 2007).

Given the placement of TM1 and TM4 in the high-resolution structures of rhodopsin (Palczewski *et al*, 2000) and the B2AR (Cherezov *et al*, 2007), it is not possible for these segments to contribute to the same dimer interface. Although not without substantial controversy (Chabre *et al*, 2003),

*Corresponding author. Center for Molecular Recognition and Departments of Psychiatry and Pharmacology, College of Physicians and Surgeons, Columbia University, 630W 168th street, P&S, Room 11-401, NY 10032, USA. Tel.: +1 21 230 573 08; Fax: +1 21 230 555 94; E-mail: jaj2@columbia.edu
[6]These authors contributed equally to this work

Received: 27 February 2008; accepted: 9 July 2008; published online: 31 July 2008

©2008 European Molecular Biology Organization

higher order packing of native rhodopsin into rows of well-organized protomers has been visualized by atomic force microscopy (AFM) (Fotiadis *et al*, 2003), and biochemical and biophysical findings in other GPCRs also suggest the possibility of higher order organization (Park and Wells, 2004; Lopez-Gimenez *et al*, 2007; Philip *et al*, 2007). A higher order organization of GPCRs could simultaneously provide for symmetrical TM1 and TM4 interfaces (Liang *et al*, 2003).

Here, we use protein complementation assays combined with resonance energy transfer to demonstrate that in living mammalian cells, the dopamine D2 receptor (D2R) is organized in a unit comprised of at least four protomers. In addition to the symmetrical interface in TM4 we established previously by Cys crosslinking, in the present work, we identified a patch of residues at a second symmetrical interface at the extracellular end of TM1. As predicted by our biophysical data, crosslinking of receptors with Cys substituted simultaneously into both TM1 and TM4 led to higher order species, consistent with a higher order organization of D2R in the plasma membrane of intact cells. The rate and extent of crosslinking were unaltered over a 100-fold range of receptor expression, suggesting that the receptor is organized into a higher order structure at physiological levels of expression.

Results

Higher order oligomerization: resonance energy transfer evidence

Given the controversy regarding the possibility that class A GPCRs are organized as higher order oligomers, we developed a biophysical approach using a combination of luminescence and fluorescence complementation and energy transfer approaches to explore the higher order structure of the D2R in living cells. First, we used bimolecular fluorescence (BiFC) (Hu *et al*, 2002) and luminescence (BiLC) (Paulmurugan *et al*, 2004) complementation assays to study the D2R dimer. Split fluorescent (or luminescent) proteins are not fluorescent (or luminescent) when expressed alone, but when fused to proteins that are located in close proximity, they can be assembled early in biosynthesis and thereby complement fluorescence (or luminescence) and report on molecular proximity (Kerppola, 2006).

Coexpression of C-terminally tagged D2R with either split monomeric Venus (mVenus) (Zacharias *et al*, 2002) (D2–V1 and D2–V2) or split *Renilla* luciferase 8 (RLuc8) (Loening *et al*, 2006) (D2–L1 and D2–L2) resulted in efficient complementation of fluorescence or luminescence, respectively (Figure 1A and C). Evidence for specificity of the interactions came from experiments using the thyrotropin receptor (TSHr) fused at its C terminus to split Venus or RLuc8. TSHr readily complemented with TSHr (data not shown), but much lower levels of heterocomplementation were observed between D2R and TSHr with either combination of constructs (Figure 1B and D).

Homogeneous time-resolved fluorescence (HTRF) experiments using probes directed against distinct N-terminal epitope tags in the split D2R constructs confirmed their interaction at the cell surface. Complementation of the split probes did not affect energy transfer (Figure 1A inset), indicating that complementation does not enhance D2R–D2R interactions. Thus, the proximity of receptors in a dimeric or oligomeric complex early in biosynthesis (Kerppola, 2006) is maintained on the plasma membrane, with or without complementation. To confirm that complementation is without impact on plasma membrane expression, we performed confocal microscopy analysis of various combinations of the transfected receptor constructs. As expected, Venus complemented by D2–V1 and D2–V2 is almost exclusively on the plasma membrane (Supplementary Figure 1c). In striking contrast, the lower levels of complementation of TSHr and D2R originate exclusively from receptor complexes that are retained intracellularly (Supplementary Figure 1c). Similar intracellular retention was observed upon coexpression of D2R–V1 and the single membrane-spanning protein CD8 fused to V2, which was tested as an additional control (Supplementary Figure 1c). We also carried out cell surface fluorescence-activated cell sorting (FACS) analysis, which indicated that any combination of TSHr and D2R that can complement (V1–V2 or L1–L2 in both orientations) leads to complete intracellular retention of TSHr (Supplementary Figure 1d inset). Thus, the low nonspecific complementation appears to result from receptors that become inappropriately attached by cotranslational folding of Venus or RLuc8, but the quality control mechanism of the cell does not allow these species to reach the cell surface.

In parallel, we also used bioluminescence resonance energy transfer (BRET) (Xu *et al*, 1999) to study receptor interactions. We performed BRET titration experiments with cells coexpressing constant amounts of D2–RLuc8 and increasing concentrations of D2–Venus (full-length versions of the previously split proteins). A specific and saturable BRET signal was observed for D2R–D2R (Figure 2A), as well as for the TSHr–TSHr (data not shown), which is known to homodimerize (Urizar *et al*, 2005). The level of BRET between D2R–RLuc8 and TSHr–Venus was low, but the expression levels of the TSHr–Venus were not sufficient to titrate fully the D2–RLuc8. To insure that the direction and the orientation of the BRET between the receptors did not affect the results and to allow full titration between TSHr and D2R, we swapped the probes and still observed very low and right-shifted BRET, which in this case was titrated fully (Figure 2A). In contrast to the hetero-complementation studies described above, TSHr–RLuc8 was seen on the plasma membrane in the presence of D2–Venus (data not shown).

To confirm the specificity of these interactions, to rule out a role of the biosensor orientation and to avoid biased comparisons between different BRET couples, we performed BRET experiments in the presence of different concentrations of untagged receptor, which would be expected to inhibit the BRET signal by competing for dimerization with the receptors fused to the probes. To ensure that the signal was consistent over the entire range of coexpression, we performed these experiments over a wide range of donor concentrations. Coexpression of untagged D2R decreased the BRET signal, whereas coexpression of TSHr or CXCR4 was without effect (Figure 2B). Competition over the entire titration range rules out changes in the absolute or relative levels of expression of the BRET probes as the cause of the decreased BRET signal (Figure 2B and C). The decrease in maximal BRET, without an associated increase in $BRET_{50}$, suggests caution in the use of $BRET_{50}$ analysis in studying receptor interactions that might be stable.

 ©2008 European Molecular Biology Organization

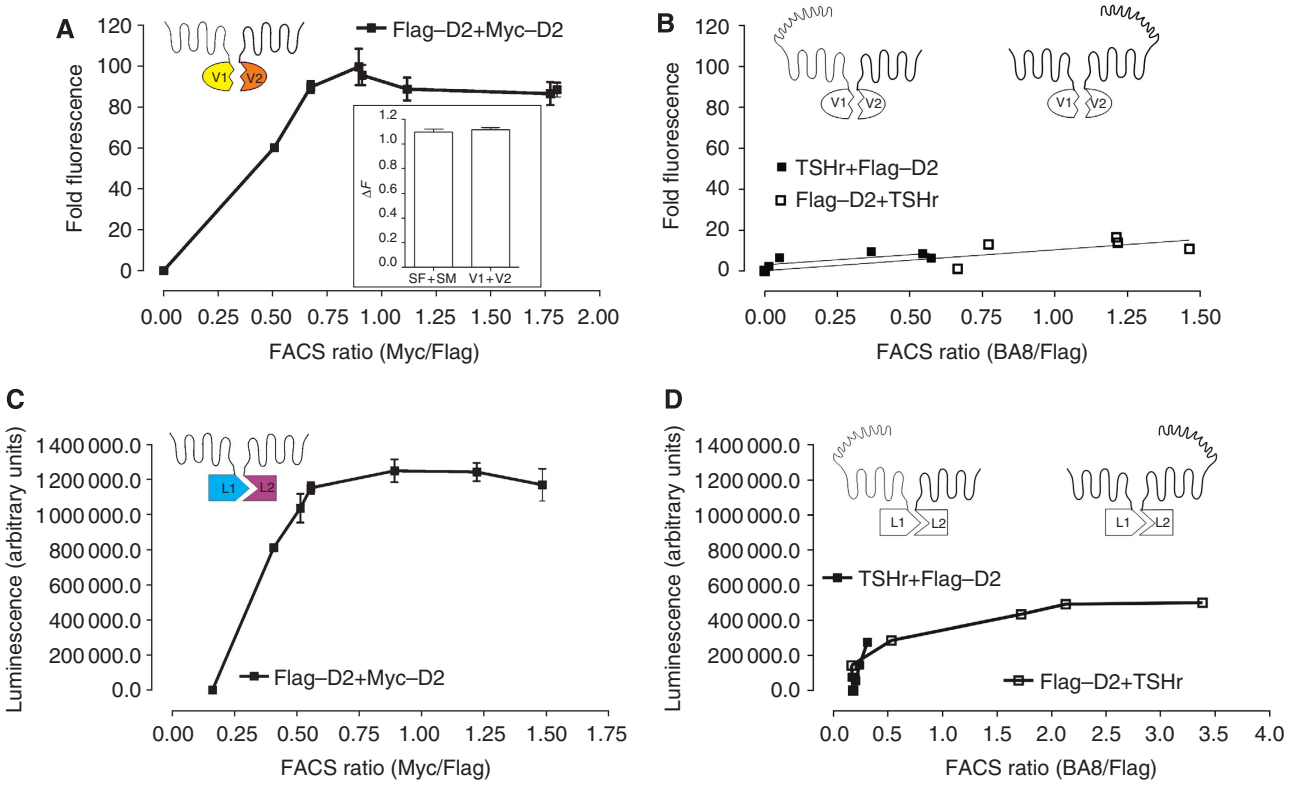

Figure 1 D2R 'dimerization' as assessed by protein complementation. HEK 293T cells transiently coexpressing D2R split Venus (**A**) or RLuc8 (**C**) or D2R and the corresponding TSHr splits (**B**, **D**) were harvested 48 h post-transfection, washed with PBS, centrifuged and resuspended in PBS. Fluorescence was recorded for 1 s using 500 nm excitation and 540 nm emission filters (Polarstar, BMG). Unfiltered luminescence was recorded for 1 s (Gain 3900). Background was determined with cells expressing only one of the receptor probes and the signal to background ratio was plotted against the FACS ratio (A–D). For the FACS ratio, cells transfected in parallel were labelled with primary and secondary antibodies (Abs) as described previously (Costagliola *et al*, 1998) and in the Methods. Relative staining for each receptor was determined independently in the same cells with the same secondary anti-mouse Ab to determine the FACS ratio. Representative results from at least three independent experiments are shown. Inset in (A) illustrates HTRF experiments performed in cells expressing identical amounts of D2–V1 and D2–V2 as compared with SF–D2 and SM–D2, respectively.

Thus, BiFC, BiLC, HTRF and BRET assays all were consistent with the robust formation of D2R 'dimers', although, one can only infer from these parallel approaches that the receptor forms at least a dimer. Once we established the basic 'dimeric' unit, we combined the different constructs to probe the existence of higher order oligomeric complexes in living cells. Complementing RLuc8 with coexpression of D2–L1 and D2–L2 resulted in a very efficient donor for the full-length D2–Venus but not for the TSHr–Venus (Figure 2D). As for the full-length BRET (see above), only the complemented RLuc8 generated by coexpressing D2–L1 and D2–L2 was a donor for D2–Venus and none of the other combinations assayed substituting L1, L2 or both with TSHr–splits gave significant BRET signals (Supplementary Figure 2a and b).

Similar results were obtained expressing constant amounts of D2–RLuc8 full-length construct as donor with the split acceptor constructs, mVenus (D2–V1 and D2–V2) (Figure 2E; Supplementary Figure 2c). All the tested probes were expressed and functional (Supplementary Figure 1a and b) and transfections were adapted so that the relative expression levels would be comparable. Although the TSHr constructs could not be combined with the D2R constructs to produce 'three-protomer' BRET, under similar conditions, BRET was readily observed when all the probes were attached to TSHr (Supplementary Figure 2b). In summary, when the three probes were all from D2R or all from TSHr, regardless of which reporter was split, BRET was most efficient, whereas the titration curves were right shifted dramatically when one of the protomers was substituted by the other receptor. This set of experiments confirms that D2R can form higher order complexes containing at least three receptors.

To establish that the minimum oligomeric unit is formed by at least four receptors, we carried out experiments in which both the donor and the acceptor were split and complemented. We coexpressed constant amounts of split RLuc8 (D2–L1 and D2–L2) with increasing amounts of split mVenus (D2–V1 and D2–V2), and we detected specific and saturable energy transfer between the complemented probes used as donor and acceptor, respectively (Figure 2F). Again, when any of the four probes was substituted by a homologous TSHr probe, the BRET curves were dramatically right shifted. It is important to note that complementation of either luminescence or fluorescence requires that the RLuc8 or Venus be assembled early in biosynthesis. Therefore, given the enormous number of 'non-productive' receptor combinations that would fail to show fluorescence or luminescence, or would show luminescence and/or fluorescence but not BRET (Supplementary Figure 5), our observation of a substantial 'four-protomer BRET' signal is remarkable. Our demonstration of resonance energy transfer between the

©2008 European Molecular Biology Organization

complemented RLuc8 and the complemented Venus shows that at least four receptors are located in close molecular proximity in living cells.

A patch of residues at the extracellular end of TM1 forms a second symmetric dimerization interface

We had previously identified a site of symmetrical interaction in TM4 of D2R (Guo *et al*, 2003, 2005), but the energy transfer data described above imply the existence of another interface. A molecular model proposed based on the AFM data of native murine rhodopsin (Fotiadis *et al*, 2003; Liang *et al*, 2003) placed a second symmetrical interface in TM1, and we therefore first focused on this region. In our background D2R construct (see Methods), the endogenous Cys168$^{4.58}$ at the TM4 interface is mutated to Ser to eliminate crosslinking (Guo *et al*, 2003). In this background, we mutated each residue in TM1 to Cys, one at a time, from the extracellular end (P32$^{1.30}$) to the beginning of the putative first intracellular loop (R61$^{1.59}$) and stably expressed these mutants in HEK 293 cells. On the basis of immunoblotting, 28 of the mutant receptors were well expressed and maturely glycosylated, whereas mutation to Cys of the highly conserved residue N52$^{1.50}$ led to loss of immunoreactivity (Figure 3A and B). Of the 28 Cys mutants that were expressed, treatment

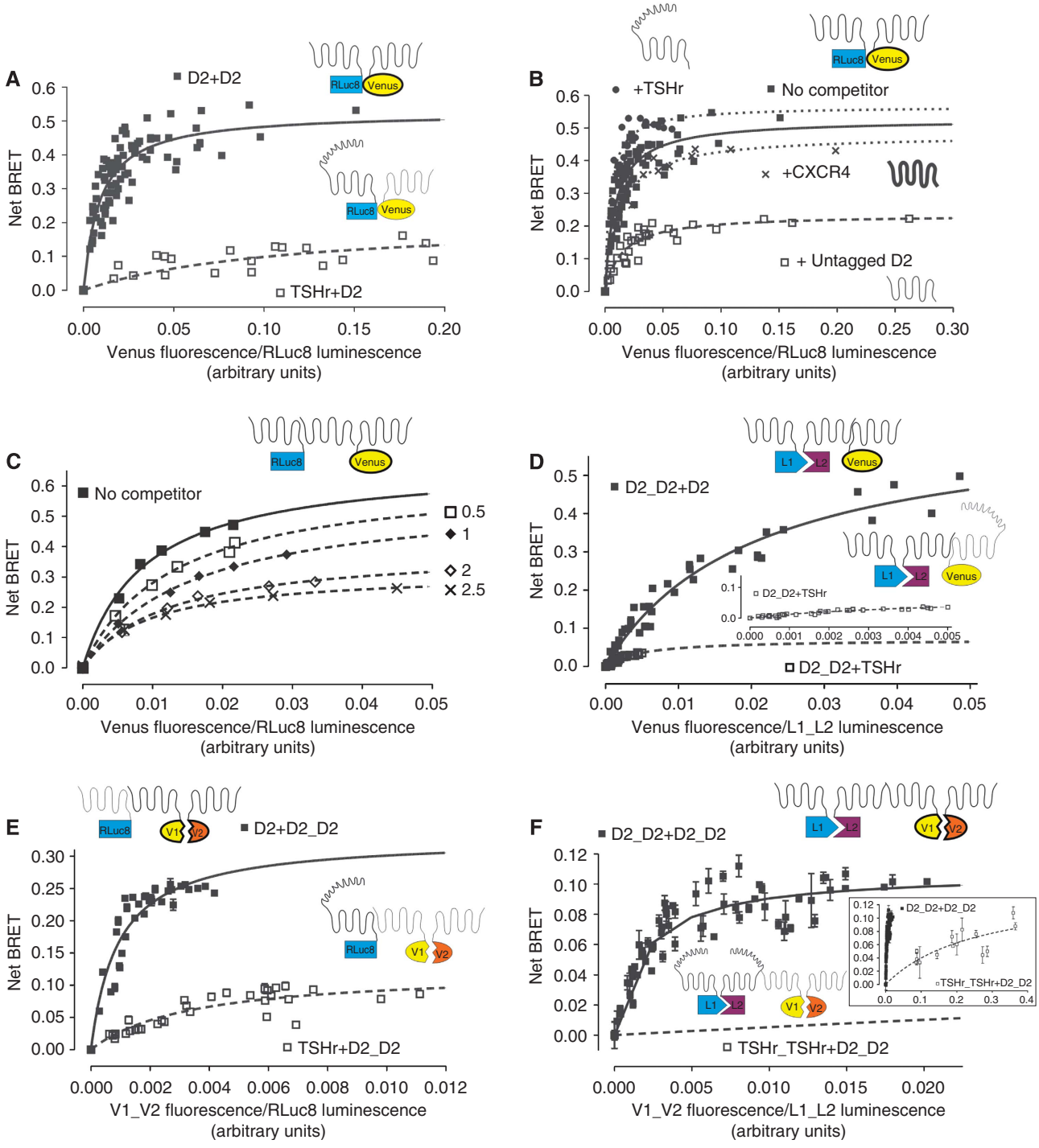

©2008 European Molecular Biology Organization

with 1 mM copper phenanthroline (CuP) led to oxidative crosslinking of four mutants ($Y36^{1.34}C$, $Y37^{1.35}C$, $L40^{1.38}C$ and $L43^{1.41}C$) to a species with a mobility on SDS–PAGE consistent with that of a D2R dimer (Figure 3A and B), as we observed previously with selected Cys in TM4 (Guo *et al*, 2005). To estimate the susceptibilities to crosslinking, we

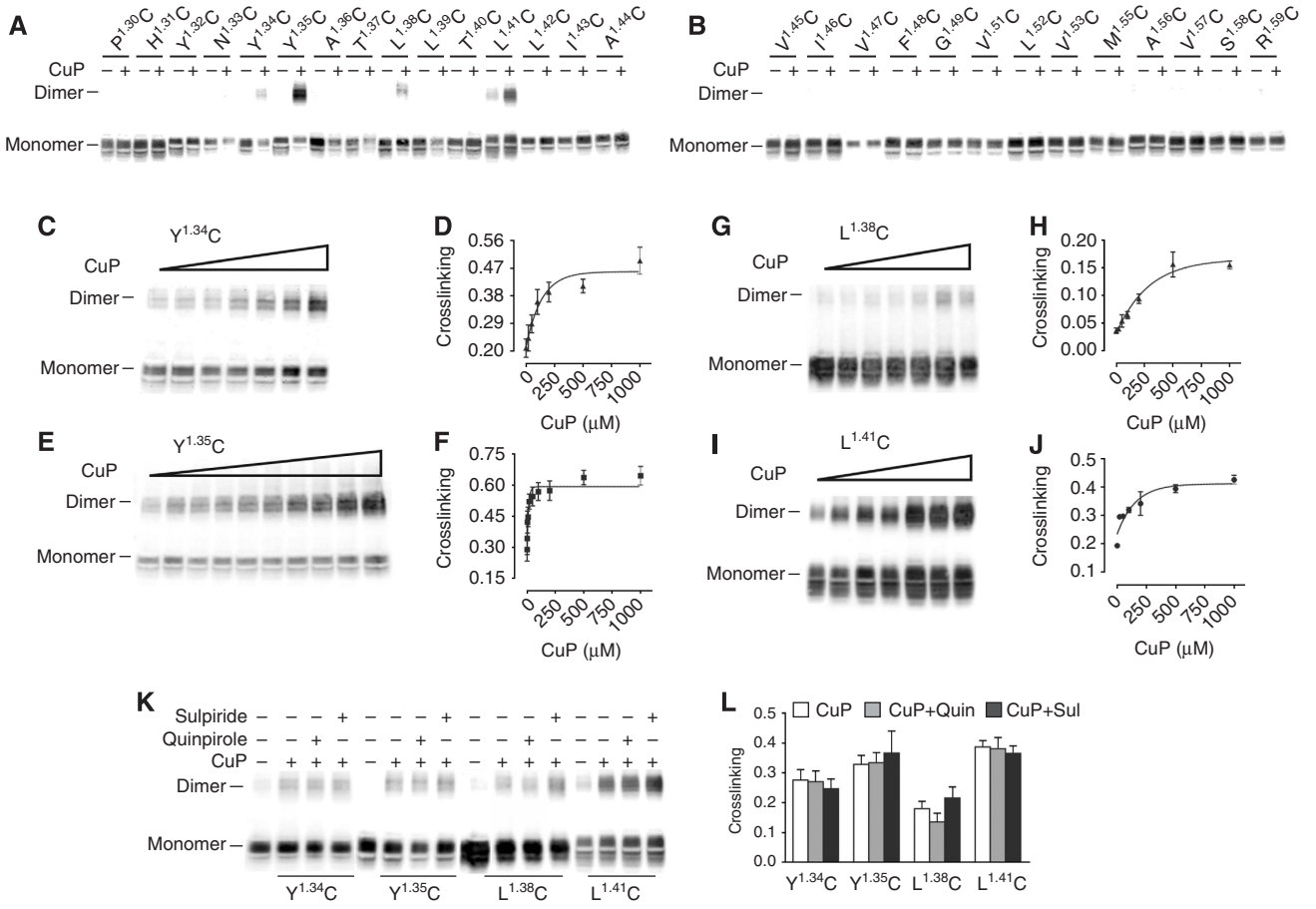

Figure 3 TM1 forms a symmetrical 'dimerization' interface in D2R. (**A**, **B**) Intact cells stably expressing substituted Cys mutants in TM1 from $P32^{1.30}C$ to $R61^{1.59}C$ (denoted using the indexing system described in Methods) (except for non-expressed $N52^{1.50}C$ and the endogenous $C56^{1.54}$, which is present in the background construct and all the mutants) were treated with 1 mM CuP in a 1:2 molar ratio at 25°C for 10 min, washed with PBS buffer, treated with NEM and analysed by immunoblotting. (**C**–**J**) Crosslinking was performed as described above with increasing concentrations of CuP for the four Cys mutants of interest $Y36^{1.34}C$ (C, D), $Y37^{1.35}C$ (E, F), $L40^{1.38}C$ (G, H) and $L43^{1.41}C$ (I, J). The dimer fraction is plotted against CuP concentration to determine the apparent crosslinking rates and efficiency. (**K**, **L**). Intact cells were treated with 1 mM CuP for $Y36^{1.34}C$, $L40^{1.38}C$ and $L43^{1.41}C$ and 5 μM for $Y37^{1.35}C$ in the absence or presence of 10 μM sulpiride or 10 μM quinpirole. Quantification of crosslinking fractions was performed as described in Methods. All experiments were repeated ⩾3 times, and one representative experiment is shown.

Figure 2 Biophysical evidence of higher order oligomerization. (**A**) Two-protomer BRET: increasing amounts of D2–Venus were coexpressed with constant amounts of either D2–RLuc8 or TSHr–RLuc8 in HEK 293T cells. At 48 h post-transfection, BRET was performed and the BRET signals were plotted against the relative expression levels of each tagged receptor. Results were analysed by nonlinear regression assuming a model with one site binding (GraphPad Prism 4.0) on a pooled data set from four independent experiments. (**B**) BRET was performed as described above in cells coexpressing constant amounts of D2–RLuc8 and increasing amounts of D2–Venus in the absence (■ and solid line), or presence of three different class A GPCRs (D2R: □ and dashed line; TSHr: ● and dotted line; CXCR4: × and dotted line). Cell surface expression of each untagged receptor used as a competitor was monitored by FACS (not shown). As above, pooled BRET signals from three independent experiments were plotted against relative expression ratios assuming a one-binding site model. (**C**) BRET assay was performed in cells coexpressing constant D2–RLuc8 and increasing D2–Venus with increasing amounts of untagged D2R as described above. The increasing level of surface expression of the competing D2R and surface expression of TSH and CXCR4 was confirmed by FACS (data not shown). A representative experiment performed three times is shown. (**D** and inset) Three-protomer BRET: cells coexpressing constant amounts of D2–L1 and D2–L2 as a BRET donor (complemented RLuc8) and increasing amounts of either D2–Venus or TSHr–Venus as the acceptors were treated and analysed identically as described in (A). Data from a pooled data set from four independent experiments are shown. (**E**) Three-protomer BRET: cells coexpressing increasing amounts of D2–V1 and D2–V2 as the BRET acceptor (complemented mVenus) and either D2–RLuc8 or TSHr–RLuc8 as donors were treated and analysed identically as described in (A). Data from a pooled data set from four independent experiments are shown. (**F** and inset) *Four-protomer BRET*: Cells coexpressing increasing amounts of D2–V1 and D2–V2 as the BRET acceptor (complemented mVenus) and constant amounts of either D2–L1 and D2–L2 or TSHr–L1 and TSHr–L2 as donors (complemented RLuc8) were treated and analysed identically as described in (A). Data from a pooled data set from four independent experiments are shown. Cartoons represent different receptor species: D2 depicted as a 7TM alone and TSHr as the 7TM with the large extracellular domain. mVenus and the splits are represented as elliptical and RLuc8 and the splits as rectangular. In the legends, + separates donor (first) from the acceptor (second) and _ indicates the complemented pairs.

©2008 European Molecular Biology Organization

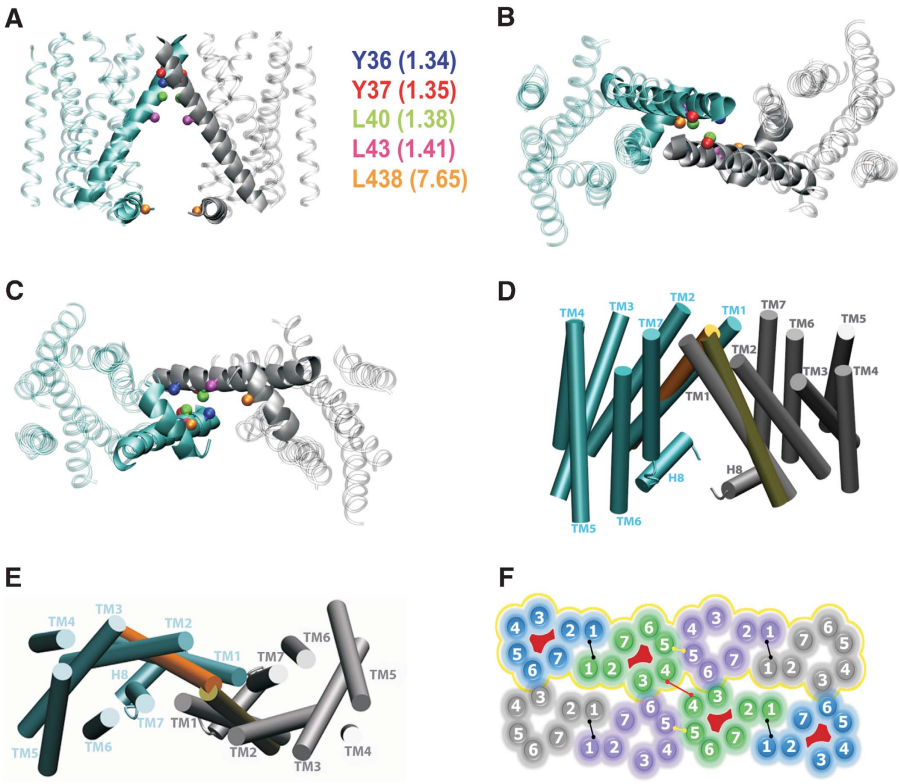

Figure 4 Molecular model of the TM1 interface and of a D2R oligomeric arrangement. Ribbon representations of (**A**) vertical, (**B**) extracellular and (**C**) cytoplasmic views of the proposed TM1–TM1 interacting regions of the D2R homodimer. The TM1 and H8 helices at the interface are highlighted by thicker traces. The Cβ atoms of residues that crosslink when mutated to Cys are shown in CPK representations in different colours. (**D**) Vertical and (**E**) extracellular views of the best fit between rhodopsin-based models of the D2R protomers (only TM1 helices are shown; orange and yellow colours) and the proposed B2AR-based model of the TM1–TM1 homodimer of D2R (cyan and grey colours). (**F**) Schematic representation of a possible D2R oligomeric organization based on inferences from our crosslinking studies (see Methods). Eight protomers are shown. The four protomers with red in the interior can be crosslinked in the $^{1.35}C/^{4.58}C$ construct. The four protomers contained in the yellow contour can be crosslinked in the $^{1.35}C/^{5.41}C$ construct (see Discussion).

treated the mutants with a range of CuP concentrations. As shown in Figure 3, the crosslinking was saturable at all four positions, with different susceptibilities to crosslinking and different maximal crosslinking (Figure 3C–J). The mutant $Y37^{1.35}C$ was the most susceptible to crosslinking (Figure 3E and F).

To explore the potential effect of ligand binding on the TM1 interface, we treated each of the four mutants with a non-saturating concentration of CuP in the presence and absence of either agonist or antagonist. In contrast to our findings in TM4 (Guo *et al*, 2005), we did not see a significant effect of these ligands on crosslinking of any of the TM1 Cys mutants (Figure 3K and L).

These data suggest that a patch of residues near the extracellular end of TM1 contributes to a symmetrical interface that does not appear to undergo major conformational changes upon ligand binding. Consistent with our predictions (Shi *et al*, 2001), the recent high-resolution structure of the B2AR (Cherezov *et al*, 2007), which has much greater sequence similarity with the D2R, showed that the greatest divergence between rhodopsin and the B2AR structure is the presence of a much straighter TM1 in B2AR. We built a homology model of the D2R based on the B2AR structure (see Materials and methods), and packed the TM1 interface to satisfy our crosslinking data (Figure 4). The same packing is not possible in the rhodopsin model, as the TM1 helices would clash in such a configuration (Figure 4D and E).

The configuration that was most compatible with our observed TM1 crosslinking places helix 8 (H8) in direct interaction with H8 from the adjacent protomer (see Discussion). In an attempt to validate this prediction, we created a series of Cys mutations ($F437^{7.64}C$, $L438^{7.65}C$ and $K439^{7.66}C$) in H8 and stably expressed these in HEK 293 cells. In intact cells, no crosslinking of the H8 Cys mutants was observed with CuP treatment (data not shown). In contrast, treatment with the membrane permeant crosslinker $HgCl_2$ led to crosslinking of $L438^{7.65}C$, consistent with the prediction of our model of the TM1 interface (Figures 4A–C and 5C). Thus, based on the biochemical and computational data, we infer that H8 is part of the symmetrical TM1 interface.

Higher order oligomerization: crosslinking evidence

Our biophysical data supporting a complex of at least four receptors and our findings of symmetrical interfaces both in TM4 and in TM1 are not compatible with a simple dimeric configuration. Moreover, the TM1 and TM4 interfaces cannot participate in forming the same symmetric interface given their distinctly different positions in the helix bundle (Figure 4F). We hypothesized, therefore, that they represented two different interfaces and that a higher order oligomeric species would be revealed by crosslinking of both TM1 and TM4 when substituted Cys were combined in the same polypeptide. To test this prediction, we stably expressed a double Cys mutant D2R that contained $Y37^{1.35}C$

 ©2008 European Molecular Biology Organization

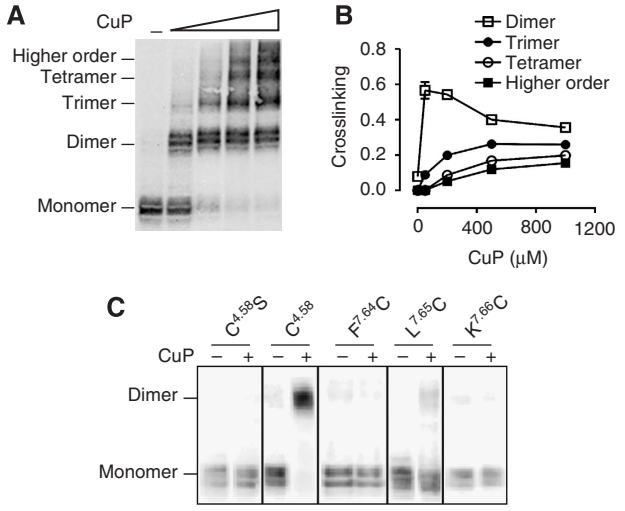

Figure 5 TM1 and TM4 contribute to symmetrical interfaces in higher order D2R complexes. (**A**) Intact cells stably expressing a D2R TM1–TM4 double Cys mutant with both TM1 $Y37^{1.35}C$ and the endogenous TM4 $C168^{4.58}$ were treated with increasing concentrations of CuP as described in Figure 3. A representative blot is shown with the different species as determined by the mass molecular weight standards. (**B**) Fractions of the different species at the indicated CuP concentration from three independent experiments (mean ± s.d.). (**C**) Intact cells stably expressing $F437^{7.64}C$, $L438^{7.65}C$ or $K439^{7.66}C$ in H8 and $C168^{4.58}$ or $C168^{4.58}S$ (as positive and negative control, respectively) were treated with 20 μM $HgCl_2$ at 25°C for 10 min and were prepared and immunoblotted as described in Figure 3. All the experiments were performed ⩾3 times, and a representative experiment is shown.

in TM1 and the endogenous $C168^{4.58}$ in TM4. Increasing concentrations of CuP resulted in the formation of higher order species (Figure 5A and B). As expected, in the presence of increasing CuP, the fraction of the receptor crosslinked to dimer decreased, whereas trimeric, tetrameric and higher order oligomeric structures increased. These data further support the existence of a higher order oligomeric organization of the D2R. Such a higher order organization is reminiscent of the arrays of rhodopsin visualized by AFM (Fotiadis *et al*, 2003; Liang *et al*, 2003), but the differences we observed in the TM1–TM1 interface suggest a somewhat different organization of the oligomeric array (Figure 4F) (see Discussion).

D2R crosslinking is independent of the level of expression

Most of the data in the literature supporting GPCR dimerization come from high-level expression in heterologous cells, although there are a limited number of cases where receptor interactions have been shown in native tissue (reviewed in Pin *et al*, 2007). To establish that our results are not specific to HEK 293 cells and that D2R oligomerization also occurs in cells that natively express D2R, we expressed the TM1–TM4 double Cys construct $Y37^{1.35}C$–$C168^{4.58}$ in CAD cells, a catecholaminergic cell line that natively expresses D2R (Pasuit *et al*, 2004). Crosslinking experiments led to higher order species (Supplementary Figure 3), just as we observed in the HEK 293 studies described above. One potential caveat of our findings and of nearly all studies of GPCR dimerization/oligomerization is that high-level expression might increase receptor interactions through molecular crowding. Importantly, 'type 2 BRET experiments' (James *et al*, 2006) in a number of GPCRs including D2R (Salahpour and Masri, 2007) support the specificity and non-collisional nature of our BRET results and a similar analysis of our BRET data leads to the same conclusion. We also observed no effect of crosslinking $C168^{4.58}$ on either the $BRET_{50}$ or maximal BRET signal (Supplementary Figure 1e), which also argues for the non-collisional nature of the BRET results. Nonetheless, to address further this potential caveat, we expressed three different receptor mutants, $Y37^{1.35}C$ in TM1, $C168^{4.58}$ in TM4 and the TM1–TM4 double Cys construct $Y37^{1.35}C$–$C168^{4.58}$, in the Flp-In T-REx system (Materials and methods). This system facilitates the rapid and reproducible creation of highly consistent pools of stable HEK 293 cells expressing different D2R mutants under the control of tetracycline (tet). This allowed us to vary the level of D2R surface expression by controlling the time of tet induction (see Materials and methods). The level of expression of the mutant receptors increased significantly with increasing tet induction time ((in femtomole per milligram membrane protein) from 81 ± 45 to 11 406 ± 1 (141-fold increase) for $C168^{4.58}$ (Figure 6A–C), from 106 ± 30 to 10 863 ± 1591 (102-fold increase) for $Y37^{1.35}C$ (Figure 6D–F) and from 106 ± 21 to 13 085 ± 646 (123-fold increase) for $Y37^{1.35}C/C168^{4.58}$ (Figure 6G–I)) (see Materials and methods). In mouse brain, the density of D2R in striatum is approximately 500 fmol/mg membrane protein (Kellendonk *et al*, 2006), well within the range explored here. Crosslinking of the individual TM1 and TM4 interfaces with saturating concentrations of CuP resulted in a constant fraction of crosslinking (Figure 6A–F) over the entire range of receptor expression studied. To examine further the impact of expression level, we performed crosslinking experiments with increasing concentrations of CuP in intact cells expressing the single TM1 or TM4 mutants 4 and 21 h after tet induction (Figure 6J–Q). For the TM1 Cys mutant, the apparent rate of crosslinking was similar at these extremely different levels of expression (Figure 6N–Q). For the TM4 Cys mutant, crosslinking was slightly more efficient for the cells expressing lower D2R amounts (4 h tet induction) (Figure 6J–M). Thus, the rates and extents of crosslinking of Cys at the TM1 and TM4 interfaces are very similar over approximately a 100-fold level of expression.

To determine the effect of expression level on the formation of higher order D2R species, we determined maximal crosslinking in the TM1–TM4 double Cys mutant $Y37^{1.35}C$–$C168^{4.58}$ expressing cells with varying tet induction times leading to a greater than 120-fold range of receptor expression (Figure 6G–I). Consistent with our findings at the individual TM1 and TM4 interface described above, in the double mutant the fraction of dimer, trimer, tetramer and higher order species was similar over the entire range of receptor expression (Figure 6I). In addition, the rate of crosslinking to higher order species was very similar at the two different levels of expression (Supplementary Figure 4).

If crosslinking between receptors resulted from random collisions, then the rate of crosslinking should be dependent on the level of expression. In contrast, we observed that the rate of crosslinking of the TM1 and TM4 interfaces was independent of the expression level (Figure 6; Supplementary Figure 4). This requires that the protomers be preorganized in the plasma membrane at physiologically relevant concentrations.

©2008 European Molecular Biology Organization

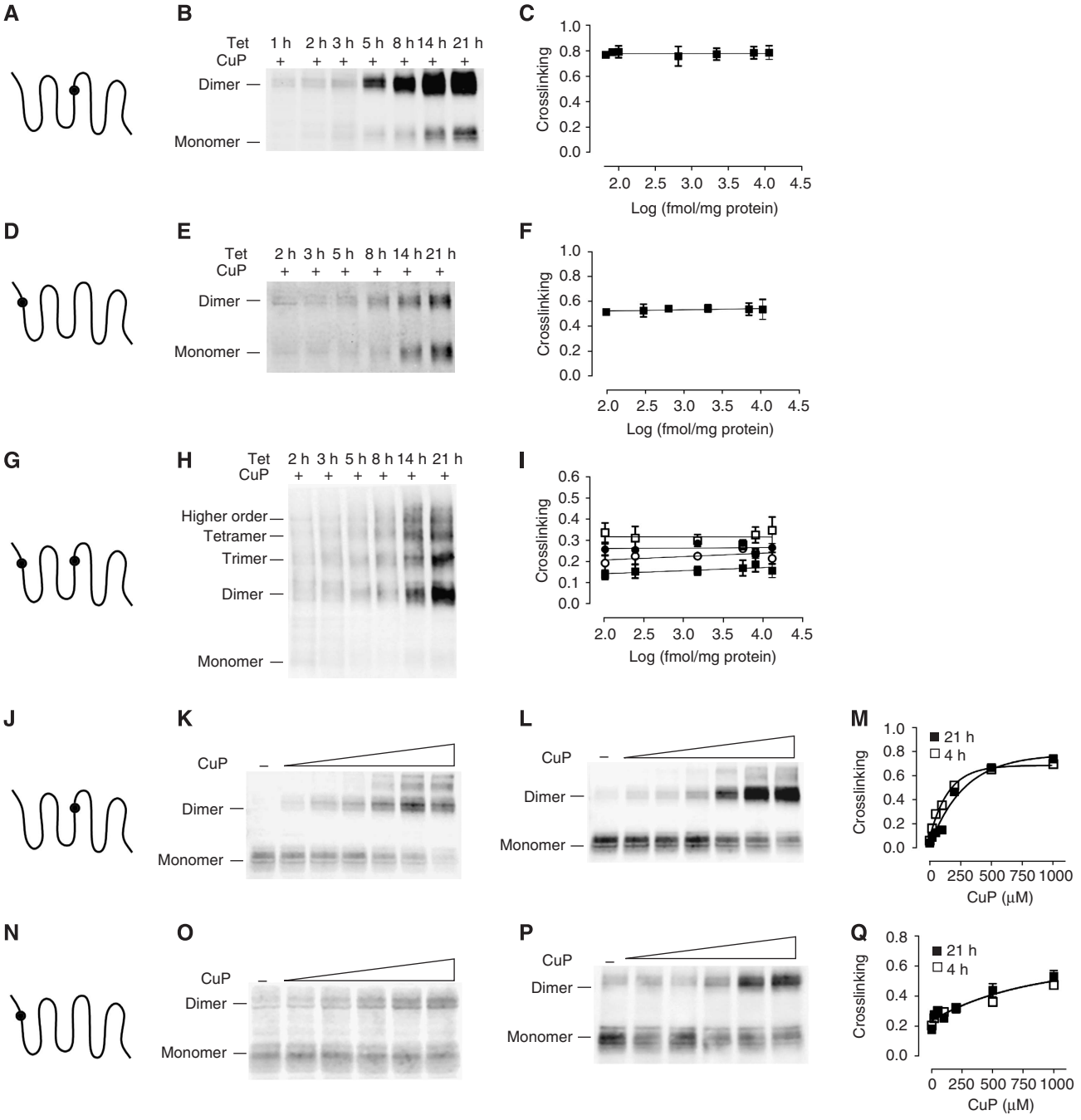

Figure 6 D2R crosslinking at physiologically relevant expression levels. HEK 293 T-rex cells were induced with 1 μg/ml tetracycline for the indicated times and Cys crosslinking was performed in cells expressing a substituted Cys at position 4.58 in TM4 (**A**–**C**), 1.35 in TM1 (**D**–**F**), or and both 1.35 and 4.58 (**G**–**I**). The experiments were performed as described for Figure 3. The fraction of immunoreactivity crosslinked to dimer (C, F) or to the various higher order species (I) was unchanged over the range of induction times, as shown by linear regression fitting. 4.58C (**J**–**M**) and 1.35C (**N**–**Q**) were induced for 4 h (K, O) or 21 h (L, P) and the cells were treated with increasing concentrations of CuP. Nonlinear regression analysis assuming a one-phase association (Prism 4.0) of the dimer fraction against [CuP] of three independent experiments (M, Q) is shown. Representative blots, in each case from three independent experiments, are shown.

Discussion

By combining luminescence and fluorescence complementation with energy transfer studies, we have established that the minimal unit for receptor organization in the plasma membrane is four protomers. In addition, by placing Cys simultaneously at TM1 and TM4 we detect crosslinking of four or possibly more receptors in a complex. Moreover, we have been able to delineate the TM segments that participate in two symmetric interfaces in these receptor complexes in the membrane environment.

Several reports suggest that GPCRs not only dimerize but also form higher order complexes or oligomers (Park and Wells, 2004; Lopez-Gimenez *et al*, 2007; Philip *et al*, 2007). AFM of native rhodopsin has directly supported such an organization (Fotiadis *et al*, 2003; Liang *et al*, 2003), although these observations have been the subject of substantial controversy (Chabre *et al*, 2003). Our results indicate that

 ©2008 European Molecular Biology Organization

the D2R and by implication other related GPCRs do indeed form higher order complexes and most importantly that these interactions are observed at physiological levels of expression. Higher order complexes were not detected in some class C receptors but were detected in others (Brock *et al*, 2007; Maurel *et al*, 2008), and further research will be necessary to clarify which GPCRs are organized in higher order complexes. It will also be important to explore the potential role of microdomain localization, such as cholesterol-rich regions, on the organization of GPCRs into higher order oligomers (Meyer *et al*, 2006).

That we could activate D2R receptor by disulphide trapping of appropriately placed Cys substitutions in TM4 (Guo *et al*, 2005) suggests an important role of the interface in activation and a coupling between ligand binding and the conformation of the TM4 interface. In the inactive inverse agonist-bound state, crosslinking occurs at the TM4–TM5 interface, whereas, in the active state, crosslinking occurs through a different face of TM4 (Guo *et al*, 2005). Crosslinking of these different faces may reflect rotation or translation of TM4 at the interface, although such an extensive movement seems unlikely (Guo *et al*, 2005). Another potential mechanism we proposed to explain these findings was that a more subtle reorganization of an oligomeric array could alter the protomers that are crosslinked, and thereby alter the face of TM4 involved in forming the identified interface (Guo *et al*, 2005). Our current data support the existence of such a higher order organization, with symmetrical interfaces at both TM4 and TM1. Curiously, the receptor protomers can be packed into an oligomeric arrangement that is consistent with formation of an interface involving TM1, the 'active' interface in TM4, and the 'inactive' TM4–TM5 interface (Figure 4F). How accurately this model depicts the exact packing and whether these interfaces can be formed simultaneously or exist only in particular conformational states remain to be determined. Interestingly, as predicted by the model (Figure 4F), a D2R with Cys substituted for 1.35 in TM1 and 5.41 in TM5 also led to crosslinking to higher order species (data not shown) that were indistinguishable from those crosslinked in the $^{1.35}$C–$^{4.58}$C construct (Figure 5A and B).

Structural studies of the receptor–G–protein interface have led to the identification of several points of contact between the G protein and the receptor on both α- and βγ-subunits (Hamm, 2001), and in the native membrane, some of these contacts have been proposed to be contributed by a second GPCR protomer (Krzysko *et al*, 2007). Consistent with this proposal, mass analysis of crosslinked LBT4 receptor reconstituted with G protein suggested that the signalling unit is comprised of two receptors and one heterotrimeric G protein (Baneres and Parello, 2003). The nanodisc experiments (Introduction) show clearly that a second protomer is not essential for a single GPCR to activate G protein efficiently. However, when a second protomer is present *in vivo*, it could modulate G protein activation. This is particularly important for heterooligomeric signalling in which ligand binding to one protomer alters signalling through the other protomer. Indeed, ligand binding to one protomer in a GPCR dimer appears to be sufficient to cause an activation-like conformational change in the unbound protomer (Damian *et al*, 2006; Brock *et al*, 2007), consistent with transfer of information between the protomers and thus with a functional role of dimerization.

Our previous crosslinking findings established the contribution of TM4 of the D2R to a symmetric 'dimer' interface (Guo *et al*, 2003, 2005). Here, we show the existence of a second symmetrical interface in TM1, consistent with indications that TM1 may have a function in 'dimerization' in a number of other GPCRs (Overton and Blumer, 2002; Carrillo *et al*, 2004; Ruprecht *et al*, 2004; Kota *et al*, 2006; Salom *et al*, 2006). Modelling a TM1–TM1 interface of D2R homodimers based on the rhodopsin template is complex given the relatively low sequence identity in this region. Indeed, we had previously inferred that the structure of TM1 and its position within the TM bundle is likely to be quite different in the biogenic amine receptors than in rhodopsin (Shi *et al*, 2001). The recent availability of the high-resolution structure of the B2AR confirmed this hypothesis (Palczewski *et al*, 2000; Cherezov *et al*, 2007). TM1 of B2R is considerably straighter than in rhodopsin, which leads to a displacement of the extracellular end of TM1 by ∼7 Å when the Cα's of residues 1.48–1.59 in the intracellular regions are superimposed. Modelling the D2R–TM1 interface using the B2AR as a structural template, the extracellular patch of crosslinked residues in D2R is compatible with a TM1–TM1 packing interface that is not possible in a rhodopsin-based model, as the TM1 helices would clash (Figure 4D and E). This configuration also places H8 at the TM1–TM1 interface (Figure 4A and C). We tested our model with several new Cys substitutions in H8, and the crosslinking of L438$^{7.65}$C was consistent with our predictions.

Although consistent with a higher order structure with symmetric interfaces involving TM4 and TM1, in the model based on inferences from AFM of native rhodopsin (Liang *et al*, 2003; Supplementary Figure 6), different TM1 residues participate and H8 does not contribute to the interface. Moreover, the 'active' TM4 interface in this array does not appear to be sufficiently close to explain our crosslinking results. Other symmetric TM1 interfaces have been observed in crystal structures, but as both rhodopsin and B2AR are monomers in detergent, the interfaces formed upon crystallization are of uncertain relevance to native interfaces in the plasma membrane. Nonetheless, our TM1 interface is most similar to that of metarhodopsin I (Ruprecht *et al*, 2004; Supplementary Figure 6), which also places H8 at the interface, but the molecular details differ due to the more extensive kink in TM1 of metarhodopsin (Supplementary Figure 6).

In summary, we have provided evidence using independent biochemical and biophysical approaches that D2R forms higher order oligomers in living cells. We have demonstrated that this higher order organization appears to be independent of expression level over greater than a 100 fold range that includes physiological levels of expression. Furthermore, we have gained insight into the oligomer by demonstrating that TM1 and H8 form a second symmetric interface in addition to the TM4 interface that we identified previously, and we have interpreted our data in a structural context by building a model of the TM1 interface based on the recently available high-resolution structure of the B2AR. Our results are consistent with mounting evidence that in the native membrane the functional unit of a GPCR involves more than a single receptor protomer.

©2008 European Molecular Biology Organization

Materials and methods

Numbering of residues, receptor constructs and transfection

Residues are numbered both according to their positions in the human $D2_{short}$ receptor (D2R) sequence and also relative to the most conserved residue in the TM in which they are located (Ballesteros and Weinstein, 1995). The most conserved residue in each TM is assigned the position index '50', for example, in TM1, Asn-52$^{1.50}$, and therefore Gly-51$^{1.49}$ and Val-53$^{1.51}$. TM1 Cys mutations in pCIN4 were generated and confirmed as described (Guo *et al*, 2003). Each mutation was generated in an N-terminally Flag-tagged background D2R construct in which Cys-118$^{3.36}$, Cys-168$^{4.58}$, Cys-370$^{6.61}$ and Cys-372$^{6.63}$ were mutated to Ser, and stably expressing pools of HEK 293 cells were created as described (Guo *et al*, 2003). Note that the binding properties and accessibility of these Cys substitutions in a slightly different background have been characterized in detail (Shi *et al*, 2001), and a representative set of the mutants used here was shown to be activated similarly by dopamine (Supplementary Figure 1b), confirming that their folding and overall structure are expected to represent that of wild-type receptor.

Selected D2R constructs were subcloned into pcDNA5/FRT (Invitrogen) and co-transfected with the recombinase expression plasmid pOG44 in a 1:9 ratio, to make tet-inducible Flp-In T-REx-293 stable cells, through selection with 500 μg/ml hygromycin, according to the manufacturer's instructions.

For the transient expression experiments, different sensors or split sensors were subcloned into the wild-type Flag–D2R in the pcDNA 3.1 expression vector, sequenced and expressed in HEK 293T cells using polyethylenimine in a 1:3 ratio (Polysciences Inc.). The experiments were performed 48 h post-transfection. The probes (full length or splits of mVenus and RLuc8) were fused to the C terminus of the D2R with a 24 amino-acid linker between the two proteins. mVenus and RLuc8 were kindly provided by D Piston and S Gambhir, respectively. D2–V1 encodes the N-terminal split of mVenus (aa 1–155) fused to the D2R, D2–V2 expresses the D2R fused to C-terminal mVenus (156–240), D2–L1 expresses the N terminus of RLuc8 fusion (aa 1–229) and D2–L2 expresses the RLuc8 C-terminal fusion (aa 230–311). Unless otherwise specified, the D2R was N-terminally Flag tagged for cytometry experiments, to determine the receptor level of expression in the cell surface. TSHr constructs were subcloned into the TSHr–RLuc pcDNA 3.1 template kindly provided by S Costagliola. 3HA-CXCR4 in pcDNA 3.1 was from the Missouri cDNA Resource Center (www.cdna.org).

Complementation, HTRF, BRET and FACS

BiFC or BiLC complementation was performed in HEK 293T cells coexpressing the different receptor–split fusions. The cells were harvested 48 h post-transfection, washed and resuspended in PBS. Approximately 200 000 cells per well were distributed in 96-well plates and the fluorescence (excitation at 510 nm and emission at 540 nm, 1 s recording) and luminescence in the presence of 5 μM coelenterazine H (no filters, 5 min post-coelenterazine addition and 1 s recording) were quantified (Polarstar and Pherastar; BMG). In parallel, FACS was performed to determine surface expression of each receptor construct, as described (Costagliola *et al*, 1998) with the Guava Easy Cite cytometer (Guava Techonologies). Briefly, a fraction of the same cells used for complementation were harvested and incubated with anti-Flag (Sigma), anti-Myc (Hybridoma Facility, Mount Sinai, New York) or BA8 (anti-TSHr-specific monoclonal antibody kindly provided by S Costagliola, IRIBHM, Brussels, Belgium), washed and incubated with the secondary anti-mouse antibody labelled either with phycoerythrin (PE) (Invitrogen) or with double PE-AF647 (to avoid cross-contamination with Venus in the yellow channel; Invitrogen). The BRET experiments were performed as described (Urizar *et al*, 2005) with cells in suspension and were quantified with a Polastar (for full-length probes) or a Pherastar (for the experiments with the different trimers and tetramers because of its higher sensitivity) (BMG). Similar results were obtained when BRET with the full-length probes was measured using the Pherastar (data not shown). HTRF was performed as described (Urizar *et al*, 2005) with anti-Flag and anti-Myc antibodies labelled with Europium Kryptate and AF647, respectively (Cis Bio, France).

Crosslinking, drug treatment and immunoblotting

The crosslinking reagents $CuSO_4$ and 1,10-phenanthroline in a 1:2 molar ratio (CuP) or $HgCl_2$ were applied to intact adherent HEK 293 cells stably expressing the indicated Cys mutants as previously detailed (Guo *et al*, 2003, 2005). For Cys mutants inducibly expressed in Flp-In T-REx-293 cells, CuP crosslinking was carried out in the same way after inducing the receptor expression with 1 μg/ml tet for the indicated time. When indicated, the inverse agonist sulpiride (10 μM) was incubated with the cells at 37°C for 60 min before crosslinking and maintained in the buffer during crosslinking. Quinpirole (10 μM) was added for 15 s and then removed immediately before the addition of CuP as described previously for dopamine application (Guo *et al*, 2005). The crosslinking reaction was stopped by washing twice with PBS buffer and addition of 10 mM *N*-ethylmaleimide (NEM). The cells were harvested and extracted, 20 μg of protein was loaded per sample and SDS–PAGE and immunoblotting using the anti-Flag polyclonal antibody (1:10 000; Sigma) were performed as described (Guo *et al*, 2005). Crosslinking rates were calculated using GraphPad Prism 4.0 software and one-phase exponential association fits.

Quantification of induced D2R expression

Expression of the mutants in Flp-In T-REx 293 cells was modulated by increasing 1 μg/ml tet induction time. The amount of receptor in the standard D2R samples was determined by measuring the B_{max} (femtomoles per milligram membrane protein) from saturation binding with [^{3}H]*N*-methylspiperone as described (Guo *et al*, 2003). D2R samples spanning the entire expression range of induced Cys mutants were loaded for SDS–PAGE and immunoblotting and a standard curve was created relating the blot densities to standard samples of known receptor concentration using GraphPad Prism 4. The expression levels of the Cys mutants were calculated from the standard curve using the measured mutant OD loaded on the same immunoblot with the standard samples.

Homology modelling of the D2DR dimer

A three-dimensional (3D) molecular model of the TM domain of the human D2R was built using the recent crystal structure of B2AR at 2.4 Å resolution as a structural template (Cherezov *et al*, 2007). An oligomeric model of the B2AR was used as a template to build a homology model of a corresponding D2R oligomer. This oligomeric arrangement is represented in cartoon form in Figure 4F. We first built a symmetric TM4–TM5 dimeric arrangement of the B2AR (green and purple protomers) based on our crosslinking results (Guo *et al*, 2005) and the oligomeric model of rhodopsin derived from AFM (Liang *et al*, 2003). Using the Insight II User Graphical Interface (Accelrys Inc.), we translated copies of the green (becomes grey) and purple (becomes blue) protomers in opposite directions along the *x* axis to generate two symmetric TM1 interfaces, indicated in Figure 4F by the black Cβ's connected by black lines. Finally, this linear array was replicated and placed in a second row to create a symmetric TM4 'active' interface, indicated in Figure 4F by the red Cβ's connected by red lines.

A sequence alignment of 37% identity over the TM regions was used to generate 100 models of D2R oligomers using the B2AR oligomeric template described above and the *MODELLER 8v2* (Sali and Blundell, 1993) molecular probability density function, which employs methods of conjugate gradients and molecular dynamics with simulated annealing at the end of the modelling routine. The structural accuracy of the best three models as determined by the lowest MODELLER objective function value was assessed by their 3D profiles calculated with the VERIFY-3D program (Luthy *et al*, 1992).The most accurate model as judged by the highest 3D–1D averaged score was selected.

Supplementary data

Supplementary data are available at *The EMBO Journal* Online (http://www.embojournal.org).

Acknowledgements

We are very grateful to S Gambhir for providing cDNA coding for RLuc8, D Piston for mVenus, S Costagliola for TSHr and mAb

 ©2008 European Molecular Biology Organization

recognizing the TSHr, D Chikaraishi for the CAD cells, to I Migeotte for assistance with the confocal microscopy, to A Karlin, N Lambert and H Weinstein for helpful discussion and comments on the paper, and to G Schertler for providing us with the modelled coordinates of the metarhodopsin I structure. This study was supported by NIH grants DA022413 and MH54137 (JAJ) and DA017976 (MF), by NARSAD and the Lieber Center for Schizophrenia Research and Treatment, and by an EMBO Long-term Fellowship (EU).

References

Ballesteros JA, Weinstein H (1995) Integrated methods for the construction of three-dimensional models and computational probing of structure–function relations in G protein-coupled receptors. *Methods Neurosci* **25:** 366–428

Baneres JL, Parello J (2003) Structure-based analysis of GPCR function: evidence for a novel pentameric assembly between the dimeric leukotriene B-4 receptor BLT1 and the G-protein. *J Mol Biol* **329:** 815–829

Bartfai T, Benovic JL, Bockaert J, Bond RA, Bouvier M, Christopoulos A, Civelli O, Devi LA, George SR, Inui A, Kobilka B, Leurs R, Neubig R, Pin JP, Quirion R, Roques BP, Sakmar TP, Seifert R, Stenkamp RE, Strange PG (2004) The state of GPCR research in 2004. *Nat Rev Drug Discov* **3:** 574–626

Bayburt TH, Leitz AJ, Xie G, Oprian DD, Sligar SG (2007) Transducin activation by nanoscale lipid bilayers containing one and two rhodopsins. *J Biol Chem* **282:** 14875–14881

Brock C, Oueslati N, Soler S, Boudier L, Rondard P, Pin JP (2007) Activation of a dimeric metabotropic glutamate receptor by intersubunit rearrangement. *J Biol Chem* **282:** 33000–33008

Carrillo JJ, Lopez-Gimenez JF, Milligan G (2004) Multiple interactions between transmembrane helices generate the oligomeric alpha(1b)-adrenoceptor. *Mol Pharmacol* **66:** 1123–1137

Chabre M, Cone R, Saibil H (2003) Biophysics—is rhodopsin dimeric in native rods? *Nature* **426:** 30–31

Chabre M, le Maire M (2005) Monomeric G-protein-coupled receptor as a functional unit. *Biochemistry* **44:** 9395–9403

Cherezov V, Rosenbaum DM, Hanson MA, Rasmussen SGF, Thian FS, Kobilka TS, Choi HJ, Kuhn P, Weis WI, Kobilka BK, Stevens RC (2007) High-resolution crystal structure of an engineered human 2-adrenergic G protein coupled receptor. *Science* **318:** 1258–1265

Costagliola S, Khoo D, Vassart G (1998) Production of bioactive amino-terminal domain of the thyrotropin receptor via insertion in the plasma membrane by a glycosylphosphatidylinositol anchor. *FEBS Lett* **436:** 427–433

Damian M, Martin A, Mesnier D, Pin JP, Baneres JL (2006) Asymmetric conformational changes in a GPCR dimer controlled by G-proteins. *EMBO J* **25:** 5693–5702

Fotiadis D, Liang Y, Filipek S, Saperstein DA, Engel A, Palczewski K (2003) Atomic-force microscopy: rhodopsin dimers in native disc membranes. *Nature* **421:** 127–128

Guo W, Shi L, Filizola M, Weinstein H, Javitch JA (2005) From the cover: crosstalk in G protein-coupled receptors: changes at the transmembrane homodimer interface determine activation. *Proc Natl Acad Sci USA* **102:** 17495–17500

Guo W, Shi L, Javitch JA (2003) The fourth transmembrane segment forms the interface of the dopamine D2 receptor homodimer. *J Biol Chem* **278:** 4385–4388

Hamm HE (2001) How activated receptors couple to G proteins. *Proc Natl Acad Sci USA* **98:** 4819–4821

Harikumar KG, Pinon DI, Miller LJ (2007) Transmembrane segment IV contributes a functionally important interface for oligomerization of the class II G protein-coupled secretin receptor. *J Biol Chem* **282:** 30363–30372

Hebert TE, Moffett S, Morello JP, Loisel TP, Bichet DG, Barret C, Bouvier M (1996) A peptide derived from a beta(2)-adrenergic receptor transmembrane domain inhibits both receptor dimerization and activation. *J Biol Chem* **271:** 16384–16392

Hu CD, Chinenov Y, Kerppola TK (2002) Visualization of interactions among bZIP and rel family proteins in living cells using bimolecular fluorescence complementation. *Mol Cell* **9:** 789–798

James JR, Oliveira MI, Carmo AM, Iaboni A, Davis SJ (2006) A rigorous experimental framework for detecting protein oligomerization using bioluminescence resonance energy transfer. *Nat Methods* **3:** 1001–1006

Ji IH, Lee C, Song YS, Conn PM, Ji TH (2002) Cis- and trans-activation of hormone receptors: the LH receptor. *Mol Endocrinol* **16:** 1299–1308

Kellendonk C, Simpson EH, Polan HJ, Malleret G, Vronskaya S, Winiger V, Moore H, Kandel ER (2006) Transient and selective overexpression of dopamine D2 receptors in the striatum causes persistent abnormalities in prefrontal cortex functioning. *Neuron* **49:** 603–615

Kerppola TK (2006) Visualization of molecular interactions by fluorescence complementation. *Nat Rev Mol Cell Biol* **7:** 449–456

Klco JM, Lassere TB, Baranski TJ (2003) C5a receptor oligomerization—I. Disulfide trapping reveals oligomers and potential contact surfaces in a G protein-coupled receptor. *J Biol Chem* **278:** 35345–35353

Kota P, Reeves PJ, RajBhandary UL, Khorana HG (2006) Opsin is present as dimers in COS1 cells: identification of amino acids at the dimeric interface. *Proc Natl Acad Sci USA* **103:** 3054–3059

Krzysko KA, Kolinski M, Filipek S (2007) Molecular modelling of the complex of oligomeric rhodopsin and its G protein. *J Phys Condens Matter* **19:** 1–12

Liang Y, Fotiadis D, Filipek S, Saperstein DA, Palczewski K, Engel A (2003) Organization of the G protein-coupled receptors rhodopsin and opsin in native membranes. *J Biol Chem* **278:** 21655–21662

Loening AM, Fenn TD, Wu AM, Gambhir SS (2006) Consensus guided mutagenesis of *Renilla* luciferase yields enhanced stability and light output. *Protein Eng* **19:** 391–400

Lopez-Gimenez JF, Canals M, Pediani JD, Milligan G (2007) The alpha1b-adrenoceptor exists as a higher-order oligomer: effective oligomerization is required for receptor maturation, surface delivery, and function. *Mol Pharmacol* **71:** 1015–1029

Luthy R, Bowie JU, Eisenberg D (1992) Assessment of protein models with three-dimensional profiles. *Nature* **356:** 83–85

Maurel D, Comps-Agrar L, Brock C, Rives ML, Bourrier E, Ayoub MA, Bazin H, Tinel N, Durroux T, Prezeau L, Trinquet E, Pin JP (2008) Cell-surface protein–protein interaction analysis with time-resolved FRET and snap-tag technologies: application to GPCR oligomerization. *Nat Methods* **5:** 561–567, advanced online publication

Meyer BH, Segura JM, Martinez KL, Hovius R, George N, Johnsson K, Vogel H (2006) FRET imaging reveals that functional neurokinin-1 receptors are monomeric and reside in membrane microdomains of live cells. *Proc Natl Acad Sci USA* **103:** 2138–2143

Ng GYK, O'Dowd BF, Lee SP, Chung HT, Brann MR, Seeman P, George SR (1996) Dopamine D2 receptor dimers and receptor-blocking peptides. *Biochem Biophys Res Commun* **227:** 200–204

Overton MC, Blumer KJ (2002) The extracellular N-terminal domain and transmembrane domains 1 and 2 mediate oligomerization of a yeast G protein-coupled receptor. *J Biol Chem* **277:** 41463–41472

Palczewski K, Kumasaka T, Hori T, Behnke CA, Motoshima H, Fox BA, Le Trong I, Teller DC, Okada T, Stenkamp RE, Yamamoto M, Miyano M (2000) Crystal structure of rhodopsin: a G protein-coupled receptor. *Science* **289:** 739–745

Park PSH, Wells JW (2004) Oligomeric potential of the M-2 muscarinic cholinergic receptor. *J Neurochem* **90:** 537–548

Pasuit JB, Li Z, Kuzhikandathil EV (2004) Multi-modal regulation of endogenous D1 dopamine receptor expression and function in the CAD catecholaminergic cell line. *J Neurochem* **89:** 1508–1519

Paulmurugan R, Massoud TF, Huang J, Gambhir SS (2004) Molecular imaging of drug-modulated protein–protein interactions in living subjects. *Cancer Res* **64:** 2113–2119

Philip F, Sengupta P, Scarlata S (2007) Signaling through a G protein-coupled receptor and its corresponding G protein follows a stoichiometrically limited model. *J Biol Chem* **282:** 19203–19216

Pin JP, Galvez T, Prezeau L (2003) Evolution, structure, and activation mechanism of family 3/C G-protein-coupled receptors. *Pharmacol Ther* **98:** 325–354

Pin JP, Neubig R, Bouvier M, Devi L, Filizola M, Javitch JA, Lohse MJ, Milligan G, Palczewski K, Parmentier M, Spedding M (2007) International Union of Basic and Clinical Pharmacology. LXVII.

©2008 European Molecular Biology Organization

Recommendations for the recognition and nomenclature of G protein-coupled receptor heteromultimers. *Pharmacol Rev* **59:** 5–13

Ruprecht JJ, Mielke T, Vogel R, Villa C, Schertler GFX (2004) Electron crystallography reveals the structure of metarhodopsin I. *EMBO J* **23:** 3609–3620

Salahpour A, Masri B (2007) Experimental challenge to a 'rigorous' BRET analysis of GPCR oligomerization. *Nat Methods* **4:** 599–600

Sali A, Blundell TL (1993) Comparative protein modelling by satisfaction of spatial restraints. *J Mol Biol* **234:** 779–815

Salom D, Lodowski DT, Stenkamp RE, Trong IL, Golczak M, Jastrzebska B, Harris T, Ballesteros JA, Palczewski K (2006) Crystal structure of a photoactivated deprotonated intermediate of rhodopsin. *Proc Natl Acad Sci USA* **103:** 16123–16128

Shi L, Simpson MM, Ballesteros JA, Javitch JA (2001) The first transmembrane segment of the dopamine D2 receptor: accessibility in the binding-site crevice and position in the transmembrane bundle. *Biochemistry* **40:** 12339–12348

Urizar E, Montanelli L, Loy T, Bonomi M, Swillens S, Gales C, Bouvier M, Smits G, Vassart G, Costagliola S (2005) Glycoprotein hormone receptors: link between receptor homodimerization and negative cooperativity. *EMBO J* **24:** 1954–1964

Whorton MR, Bokoch MP, Rasmussen SGF, Huang B, Zare RN, Kobilka B, Sunahara RK (2007) A monomeric G protein-coupled receptor isolated in a high-density lipoprotein particle efficiently activates its G protein. *Proc Natl Acad Sci USA* **104:** 7682–7687

Xu Y, Piston DW, Johnson CH (1999) A bioluminescence resonance energy transfer (BRET) system: application to interacting circadian clock proteins. *Proc Natl Acad Sci USA* **96:** 151–156

Zacharias DA, Violin JD, Newton AC, Tsien RY (2002) Partitioning of lipid-modified monomeric GFPs into membrane microdomains of live cells. *Science* **296:** 913–916

 ©2008 European Molecular Biology Organization